Ligands with polyfluorophenyl moieties promote a local structural rearrangement in the Spinach2 and Broccoli aptamers that increases ligand affinities

SHARIF ANISUZZAMAN,[1] IVAN M. GERASKIN,[2,3] MUSLUM ILGU,[1] LEE BENDICKSON,[1] GEORGE A. KRAUS,[2] and MARIT NILSEN-HAMILTON[1]

[1]Roy J. Carver Department of Biochemistry, Biophysics and Molecular Biology, Iowa State University, Ames, Iowa 50011, USA
[2]Department of Chemistry, Iowa State University, Ames, Iowa 50011, USA

ABSTRACT

The interaction of nucleic acids with their molecular targets often involves structural reorganization that may traverse a complex folding landscape. With the more recent recognition that many RNAs, both coding and noncoding, may regulate cellular activities by interacting with target molecules, it becomes increasingly important to understand how nucleic acids interact with their targets and how drugs might be developed that can influence critical folding transitions. We have extensively investigated the interaction of the Spinach2 and Broccoli aptamers with a library of small molecule ligands modified by various extensions from the imido nitrogen of DFHBI [(Z)-5-(3,5-difluoro-4-hydroxybenzylidene)-2,3-dimethyl-3,5-dihydro-4H-imidazol-4-one] that reach out from the Spinach2 ligand binding pocket. Studies of the interaction of these compounds with the aptamers revealed that polyfluorophenyl-modified ligands initiate a slow change in aptamer affinity that takes an extended time (half-life of ~40 min) to achieve. The change in affinity appears to involve an initial disruption of the entrance to the ligand binding pocket followed by a gradual transition to a more defined structure for which the most likely driving force is an interaction of the gateway adenine with a nearby 2′OH group. These results suggest that polyfluorophenyl modifications might increase the ability of small molecule drugs to disrupt local structure and promote RNA remodeling.

Keywords: Spinach2; aptamer; kinetics; ligand; structure

INTRODUCTION

Ligand-induced changes in RNA structure and function are important aspects of cellular regulation, and their understanding is critical for the development of drugs that alter RNA function and structure in vivo. The interactions of RNAs with their target molecules frequently involve significant changes in RNA structure, even if only local. These local changes are amplified in riboswitches and other functional RNAs with resulting changes in local and global RNA structure (Mandal et al. 2004; Suess et al. 2004; Priyakumar 2010; Stoddard et al. 2010; Dethoff et al. 2012).

The paths by which structural changes occur in RNAs have not frequently been studied at the molecular level in part due to the difficulty of tracking such changes over time. Spinach and Broccoli are light-up aptamers that provide an environment conducive for an increase in ligand fluorescence when bound. As this feature is compatible with tracking aptamer binding capability over long time periods, we have investigated the interactions of a series of derivatives of the ligand, DFHBI [(Z)-5-(3,5-difluoro-4-hydroxybenzylidene)-2,3-dimethyl-3,5-dihydro-4H-imidazol-4-one], with the Spinach2 (SPN2) and Broccoli (BRC) aptamers to evaluate the stability of these molecular structures over time.

Here we describe a new interaction of two polyfluorophenyl ligands with the SPN2 and BRC that involves a local structural rearrangement reflected in a slow increase in ligand affinity and requires the presence of multiple fluorines on a benzene ring appended to the imido nitrogen of DFHBI. The rearrangement results in a remodeled local structure that involves a predicted single H-bond between the amino group of the gateway adenine and a close-by

[3]**Present address:** Regis Technologies, Inc., Morton Grove, Illinois 60053, USA
Corresponding author: marit@iastate.edu
Article is online at http://www.rnajournal.org/cgi/doi/10.1261/rna.079005.121.

2′OH group. This transition demonstrates how a small ligand can alter the local structure of a much larger, already folded, RNA. The pathway in SPN2 appears to be an initial disruption of the local RNA structure followed by relaxation to an alternative structure that involves an additional hydrogen bond between the gateway adenine and a nearby 2′ hydroxyl group. Our results suggest that drugs directed to functional RNAs are likely to be more effective in altering RNA functionality if they contained moieties such as multiply fluorinated phenyl groups with the ability to disrupt local RNA structures and promote rearrangement to new ligand-driven structures.

RESULTS

Ligand screen of SPN2 and BRC affinities

Studies of the binding affinities of the Spinach aptamer family (Spinach, SPN2, Baby Spinach, iSpinach, and Broccoli) have consistently identified an adenosine group, referred to as the "gateway adenine" or "lid layer," as important for ligand affinity (Huang et al. 2014; Warner et al. 2014; Ageely et al. 2016; Warner et al. 2017). This adenine is present in position 69 in the deposited crystal structure of SPN2 (PDBID;4TS2) and in position 71 in SPN2 due to the additional 2 bases added to the 5′ end of the RNA by the T7 polymerase during in vitro transcription. The gateway A is seen in the crystal structure very close to the imido-amino-methyl group of DFHBI, which protrudes from the SPN2 binding pocket (Fig. 1A) and is shown to make a direct contact with the methyl group of DFHBI in the crystal structure of iSpinach (Fernandez-Millan et al. 2017).

To better understand how the gateway A influences ligand affinity, a library of DFHBI derivatives was produced in which the amino methyl group was extended with a variety of phenyl and benzyl groups (synthetic outcomes in Supplemental materials). Selection of the Spinach aptamer was performed with DFHBI linked to a solid support by way of the imido nitrogen (Song et al. 2014). We have found this

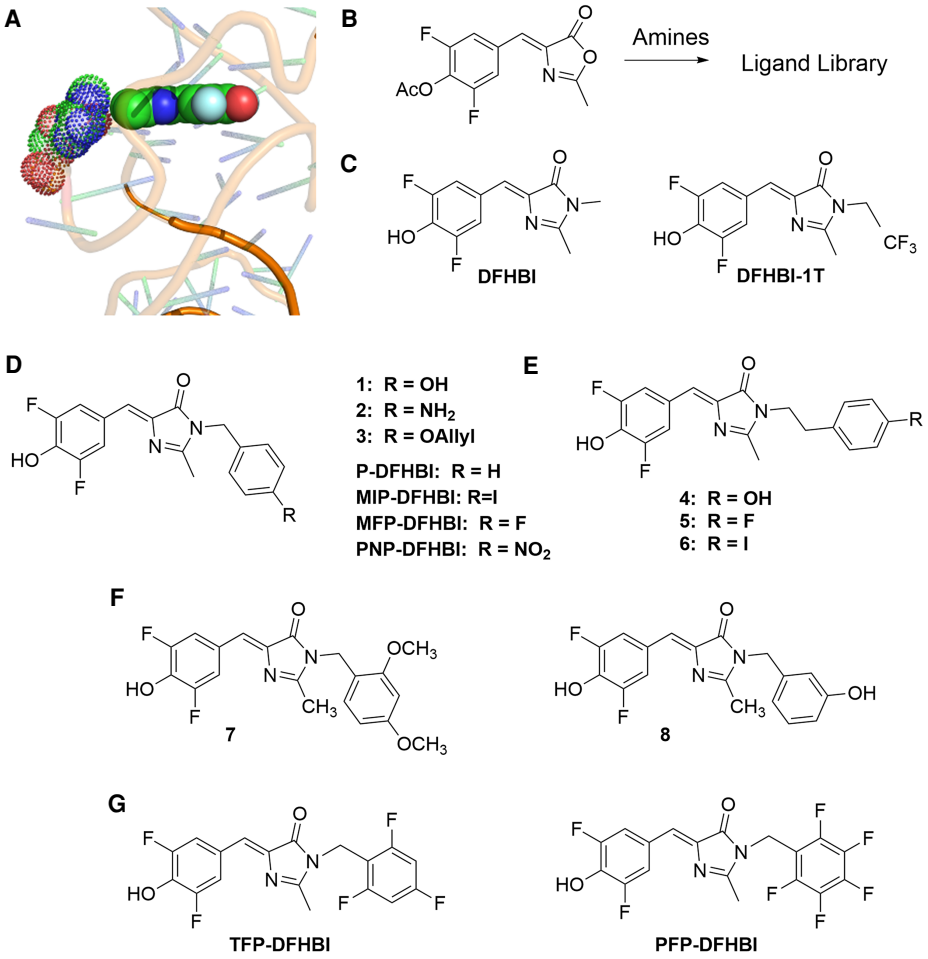

FIGURE 1. DFHBI imido-N extension library. (*A*) Positions of the gateway A (stippled) and the DFHBI methyl group (filled) SPN2 crystal structure. (*B*) Overview of the synthesis protocol for compounds. (*C–G*) Chemical structures of the synthesized DFHBI derivatives. Letter abbreviations are defined in Supplemental Table S1.

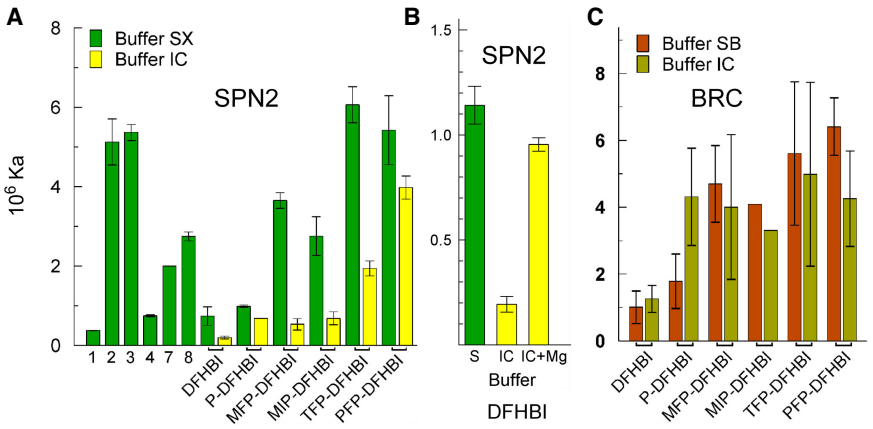

FIGURE 2. Affinities of SPN2 and BRC for imido-N extension ligands. (*A*) The affinities of SPN2 for compounds of the imido-N extension ligand library in buffer SX (green bars) or buffer IC (yellow bars) after 10 min incubation. (*B*) The effect of Mg on the affinity of SPN2 for DFHBI. Buffer IC (green bar), buffer IC with 5 mM Mg (yellow bars). (*C*) The affinities of BRC for some of the imido-N extension ligands in buffer SB (brown bars) or buffer IC (tan bars). All affinities were determined by fluorescence spectroscopy as described in Materials and Methods.

position to be optimal for modifying DFHBI while maintaining aptamer affinity for the newly synthesized modified ligands. To create the library of alternative DFHBI ligands, azlactone (Fig. 1B) was reacted with primary benzylic amines and phenethylamines. By this means, DFHBI (Fig. 1C) was modified by a variety of phenyl or benzyl groups linked to its imidazole nitrogen (Fig. 1D–G). Of these compounds, DFHBI and PFP-DFHBI have been previously reported (Paige et al. 2011; Ilgu et al. 2016). Other compounds, are either identified numerically or with letter codes if used frequently in this work. It was hypothesized that the phenyl or benzyl extensions from DFHBI might interact with the gateway A to either increase affinity by stacking or to decrease affinity by preventing the A from forming a critical interaction.

SPN2 and BRC were tested for their affinities with various members of the ligand library (Fig. 2). Although addition of the phenyl group (P-DFHBI) had a small impact on SPN2 affinity, additional constituents to the phenyl ring such as amino (compound 2), O-allyl (compound 3), and fluorine had large effects resulting in over a 20-fold range of affinities for SPN2, depending on the constituents (Fig. 2A; Supplemental Table S3).

The original Spinach aptamer was selected in buffer SX, which contains 5 mM $MgCl_2$ (Paige et al. 2011). Reports of the interaction of its derivative aptamer, SPN2, with potential ligands were performed using the same buffer but with 1 mM $MgCl_2$ (Strack et al. 2013). The binding studies shown in Figure 2A and B (green bars) were performed in buffer SX. However, in the mammalian cell, in which this aptamer has been applied, the free $MgCl_2$ concentration is about 220 µM (Romani 2013). Therefore, we also tested the binding affinity of SPN2 for the DFHBI imido-N extension library in buffer IC, formulated to resemble the salt content and pH of the mammalian cytoplasm. The results (Fig. 2A, yellow bars) show that DFHBI binds with lower affinity to SPN2 in IC buffer than in SX buffer and this difference between buffers decreases with the addition of three or five fluorines on the phenyl ring. The critical difference between buffers SX and IC for SPN2 ligand affinity is the $MgCl_2$ concentration (Fig. 2B).

BRC was selected from a Spinach aptamer-derived library in a buffer with a lower concentration of $MgCl_2$ to overcome the requirement for high Mg^{2+} (Filonov et al. 2014). BRC bound to DFHBI and derivatives equally well in both buffers SB and IC with the possible exception of P-DFHBI (Fig. 2C). Thus, for both SPN2 and BRC, the affinity for DFHBI is enhanced by the inclusion of a phenyl extension from the imido N-methyl group and is impacted by the constituent(s) on the phenyl ring.

Location of the phenyl extensions to DFHBI relative to the binding pocket

The addition of a phenyl group to DFHBI increased SPN2 ligand affinity in almost every instance (Fig. 2A). Therefore, we postulated that this group might interact with chemical groups on the aptamer near the opening of the binding pocket. If so, then the position of the phenyl group immediately outside the entry to the pocket might be important for affinity. To test this hypothesis, we prepared a series of DFHBI derivatives with benzyl extensions from DFHBI (compounds 4, 5, and 6) and compared these with their phenyl extension counterparts (compounds 1, MFP-DFHBI and MIP-DFHBI) for their abilities to bind SPN2 (Fig. 3). As well as extending further from the imido nitrogen than the phenyl extensions, the benzyl extensions were predicted to take an alternate orientation to the imidazole group when free in solution. The predominant structures of the benzyl extensions were predicted to be in plane with the imidazole group, whereas the phenyl extensions are predicted to orient in a plane almost 90° to the imidazole group (Fig. 3A). In all instances, DFHBI analogs with benzyl extensions from DFHBI had lower affinities for SPN2 than the equivalent phenyl extensions regardless of the substitution on the phenyl group (Fig. 3B). In two of the three instances, SPN2 bound the analogs with the two-carbon linkers to the imido nitrogen with lower affinity than for DFHBI, which has a methyl group at this position. These results are consistent with the hypothesis that the phenyl extension to DFHBI provides an opportunity for interaction

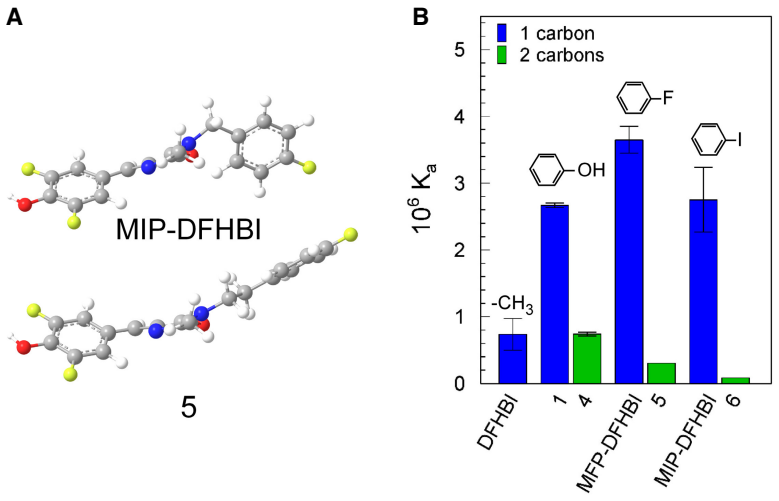

FIGURE 3. Influence of the position of the phenyl group relative to the imido nitrogen of DFHBI. (*A*) The predicted 3D models of two DFHBI derivatives with either a one carbon link to the phenyl group (MFP-DFHBI) or a two carbon link (compound 5). (*B*) Affinities (K_as) in buffer SX of compounds with benzyl or phenethyl extensions from the imido nitrogen.

of the phenyl group and its appendages with portions of the aptamer close to the binding pocket.

Time-dependent changes in SPN2 and BRC affinities

An unusual feature of the interaction of SPN2 and BRC with the DFHBI analogs containing tri- or penta-fluoro substituents was a slow increase of two- to threefold in the affinities of the aptamers for ligand over a period of hours at room temperature (22°C–24°C; Fig. 4A,B). This affinity change was unique for these two ligands and the half-life for the change was 40 ± 4.1 min ($N = 8$). The change in affinity was observed for SPN2 in IC and SX buffer and in SX buffer at pH 7.4 and 8. It was also observed for BRC in SB buffer. Although the initial affinities of SPN2 and BRC were lower for DFHBI than for PFP-DFHBI, the ability to drive a change in affinity with time was not related to the initial affinity. For example, compounds 2 and 3 bind SPN2 with similar affinities to TFP-DFHBI and PFP-DFHBI (Fig. 2A), but only the latter two ligands drive the slow change in affinity with time (Fig. 4A). To ensure that PFP-DFHBI was not changing structurally over this long incubation time, we determined its MS and UV-Vis spectra before and after repeated exposure to 485 nm over the 18 h time period. There was no change in the UV-Vis spectra over this time period (Supplemental Fig. S1). Mass spectrometry analysis showed the expected peaks after 10 min incubation with one 30 sec exposure to 485 nm light as were found after thirteen 30 sec exposures to 485 nm over a period of 18 h incubation (Supplemental Fig. S1 legend). The effect of incubation time on fluorescence in the presence and absence of SPN2 was determined for DFHBI, PFP-DFHBI, and DFHBI derivatives. Fluorescence was stable for all compounds in the absence of SPN2 but increased about 20% in the presence of aptamer for most compounds (Supplemental Table S4). The increase in fluorescence observed with DFHBI and PFP-DFHBI was identical and therefore did not contribute to the difference in measured K_a for these compounds.

To further establish the change in affinity over time with PFP-DFHBI and not DFHBI, we determined the on and off rates. These values (Table 1) confirmed that incubation of SPN2 with PFP-DFHBI but not with DFHBI resulted in a change in the kinetics of binding to the respective ligand. The calculated values of K_a for both ligands from the k_{on} and k_{off} measurements after 10 min incubation matched well with the K_as measured by fluorescence intensity. The k_{off} was measured using PNP-DFHBI to replace the exited ligand. The ratios of k_{off} (10 min) over k_{off} (18 h) were 1.2 (DFHBI) and 0.72 (PFP-DFHBI). When analyzed for statistical significance using a Student's *t*-test, the resulting *P* values were higher than 0.05. Unlike the k_{off}, which was not altered for either ligand with longer incubation nor significantly different between ligands, the k_{on} for the two ligands suggested the mechanism by which the ligand affinities are differentiated and how the SPN2 affinity for PFP-DFHBI increases with time of incubation. Whereas the calculated k_{on} for DFHBI at 18 h was 0.84 of the measured value at 10 min, it was 1.66 times the k_{on} measured at 10 min for PFP-DFHBI. This 66% change is well outside the error range of all measurements of K_a, k_{off}, and k_{on} (17% ± 8%). Thus, we conclude that difference in affinities of SPN2 for DFHBI and PFP-DFHBI and the increase in affinity of SPN2 with PFP-DFHBI with incubation is defined by the k_{on}.

The change in affinities observed with TFP-DFHBI and PFP-DFHBI occurred with the characteristics of first order reactions (Fig. 4C). This suggested a single event is responsible for shifting the aptamer into a higher affinity state. As fluorine is the constituent of both active ligands, we considered the possibility of an unusual chemical reaction causing the change in aptamer affinities. Being the most electronegative element, fluorine is not likely to be displaced from the ligand. But, fluorine can participate in H-bonds and also alters the excited electronic states of benzene by the "perfluoro effect" (Mondal and Mahapatra 2010). To investigate the possibility that the presence of fluorophenyl groups close to the aptamer might result in a covalent reaction between the aptamer and ligand or within the aptamers that lock them in a higher affinity state, we determined whether a previous

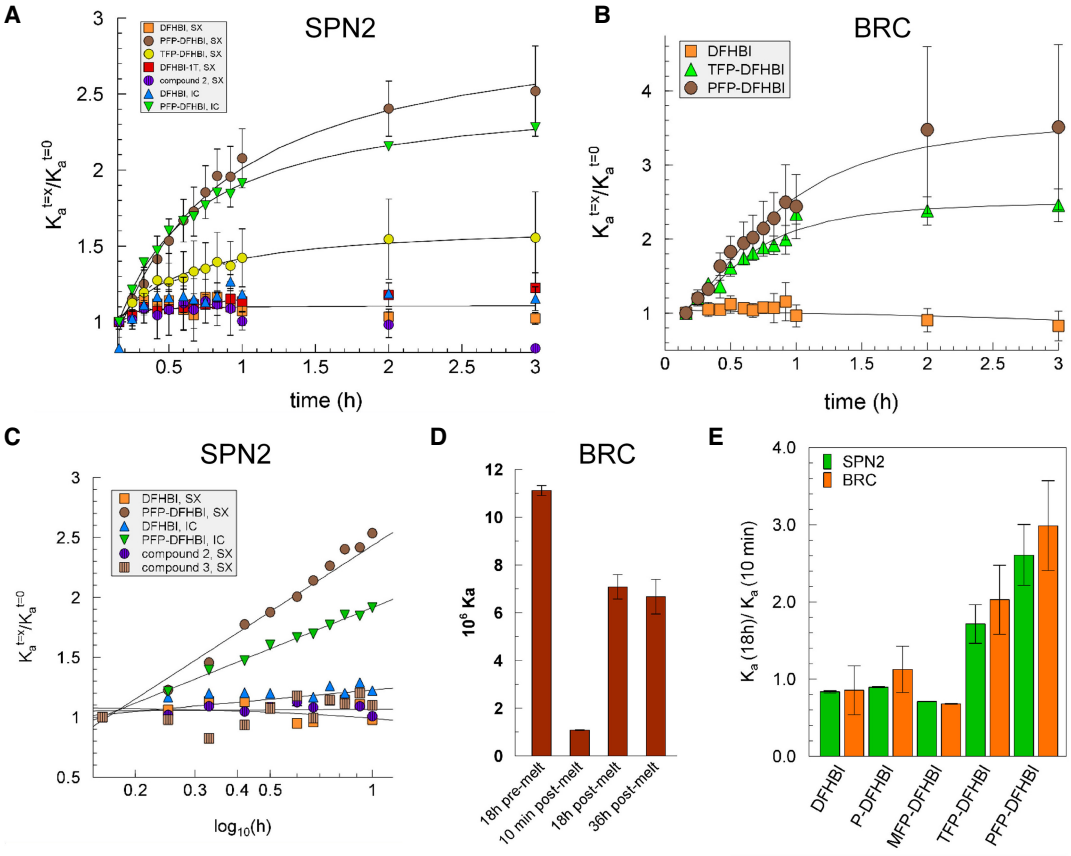

FIGURE 4. Increase in affinity with incubation time for ligands with polyfluorophenyl imido-N extensions. Affinity as a function of incubation time in the dark for (*A*) SPN2 with a variety of DFHBI derivatives in buffers identified in the legend and (*B*) Broccoli in buffer SB. (*C*) Data from *A* represented as a semi-log plot. (*D*) BRC was incubated for 18 h with PFP-DFHBI in buffer SB (18 h pre-melt), then melted at 80°C for 5 min, shifted to 23°C and the affinity measured after 10 min, 18 and 36 h post-melt. (*E*) The influence on the K_a of SPN2 and BRC of increasing numbers of fluorines on the phenyl extension.

incubation of ligand and aptamer would increase the initial affinity of the Broccoli aptamer for PFP-DFHBI (Fig. 4D). The results show that the effect of ligand on aptamer affinity does not survive a melting of the aptamer-ligand complex. Although it is possible that a heat-sensitive chemical reaction occurs to increase the affinity of these aptamers to the two ligands with the fluorophenyl appendages, we consider this an unlikely explanation for the effect of the fluorophenyl-DFHBI ligands on aptamer affinities. This conclusion is supported by the observation that DFHBI-

TABLE 1. Kinetic measurements for SPN2 interaction with DFHBI and PFP-DFHBI

Ligand	DFHBI		PFP-DFHBI	
Incubation time	10 min	18 h	10 min	18 h
K_a (μM^{-1})	0.33 ± 0.04 (2)	0.28 ± 0.30 (2)	4.0 ± 0.84 (5)	8.3 ± 1.0 (4)
k_{off} (s^{-1})	$4.9 \pm 1.2 \times 10^{-4}$ (6)	$5.8 \pm 1.3 \times 10^{-4}$ (6)	$5.3 \pm 0.15 \times 10^{-4}$ (2)	$3.9 \pm 0.15 \times 10^{-4}$ (3)
k_{on} ($\mu M^{-1}s^{-1}$)	$1.9 \pm 0.48 \times 10^{-4}$ (6)	1.3×10^{-4} (calculated)	$1.9 \pm 0.17 \times 10^{-3}$ (3)	3.2×10^{-3} (calculated)
K_a (calculated)	0.39		3.6	

k_{on} after 10 min and K_a and k_{off} after 10 min and 18 h incubation were determined for DFHBI and PFP-DFHBI. The k_{on} at 18 h was calculated from the measured K_a and k_{off}. The K_a at 10 min was also calculated from the measured k_{on} and k_{off} and found to be within 20% of the measured values for both compounds. Shown are the measured values (±SEM) with the number of independent estimates in parentheses. For k_{on}, each independent estimate involved measuring k_{obs} for at least four different ligand concentrations. For k_{off}, each independent measurement involved a duplicate measurement of the k_{off} for the same combination of ligand and aptamer with the duplicates independently constituted and analyzed for k_{off} on the same day.

1T, with a trifluoro-methyl group linked to the imido nitrogen, does not cause a change in SPN2 affinity with time (Fig. 4A).

The gateway A secondary amino group is required for increased aptamer affinity

We investigated the role of the gateway A in driving the change in affinity for the fluorophenyl DFHBI derivatives as several studies have identified it as important for DFHBI binding affinity. First, we removed the base from the gateway position 71 in SPN2. To create the apurinic SPN2 and other aptamers with alternate bases, we used the split aptamer format (Warner et al. 2014), which placed the gateway A in position 21 of one aptamer half. For replacements with natural bases, the appropriate DNA templates were used for in vitro RNA synthesis. Regardless of the moiety that replaced the gateway A, the affinity for ligands (DFHBI and PFP-DFHBI) was reduced (Fig. 5A). As for the full-length aptamer, incubation with the ligand increased the affinity of the split aptamer for PFP-DFHBI but not for DFHBI (Fig. 5B). Without the gateway base, the apurinic SPN2 bound PFP-DFHBI with about 100-fold lower affinity than with the base present and did not change in affinity for PFP-DFHBI with time (Fig. 5B,C).

The effect of ligand on aptamer affinity was compared for SPN2 with a deletion or base substitutions for the gateway A (Fig. 5C). The change in affinity with time was observed if A or C were present at the gateway position but not if G, 2AP, U, or no base were present. The results suggest that the amino group of A or C might be responsible for forming a hydrogen bond that increases stability of the binding pocket and thereby increases affinity. That SPN2 variants with bases containing a secondary amino group (but not *trans* to the glycosidic bond) did not increase in affinity with time of incubation suggests that there is a steric component to the hypothesized additional H-bond.

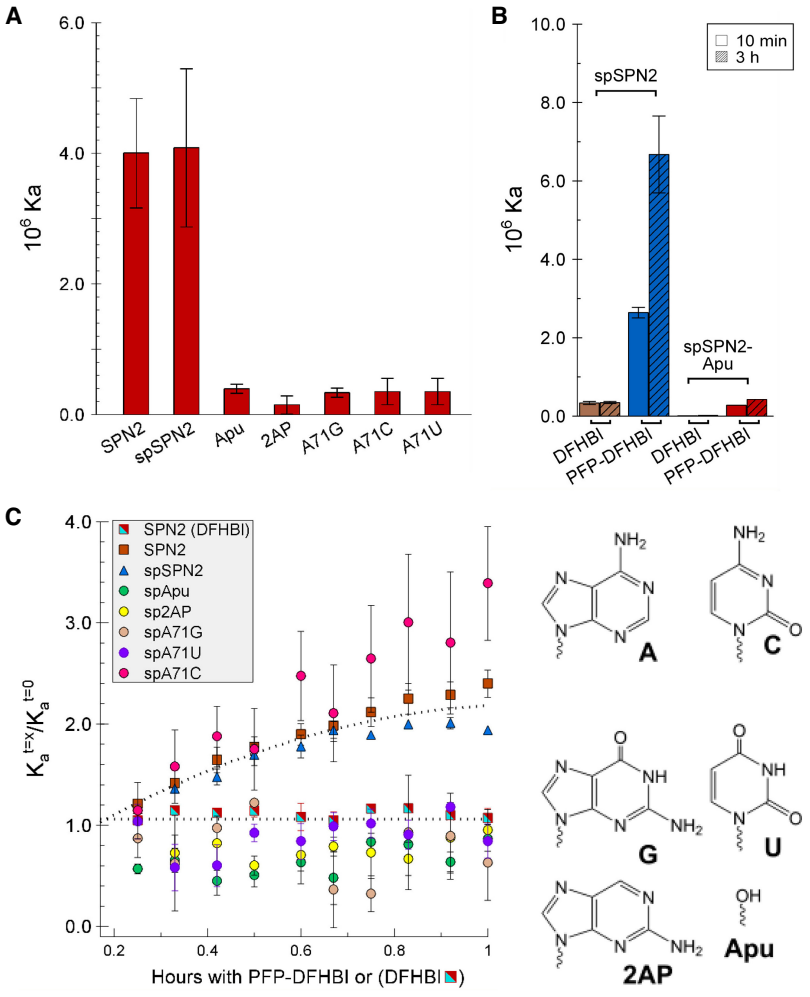

FIGURE 5. The effects of altering the gateway base on the affinity and time-dependent change in affinity of SPN2 for DFHBI and PFP-DFHBI. (*A*) Affinities after 10 min incubation for PFP-DFHBI in buffer SX of SPN2 variants in position 71 as identified in the *x*-axis labels. (*B*) Comparison of split SPN2 (spSPN2) and spSPN2 lacking a purine at position 71 (spSPN2-Apu) for their affinities for DFHBI and PFP-DFHBI after 10 min incubation (open bars) and 3 h incubation at 23°C (hatched bars) in buffer IC. (*C*) Time dependency of the affinities in buffer SX of SPN2 variants as identified in the legend. All time dependencies are for binding to PFP-DFHBI except the one identified as SPN2 (DFHBI). The glycosidic bond is represented by the squiggle in each chemical structure. Each data set is from a titration performed as a single experiment and identified with a different color. Each titration was performed independently two to four times with duplicate samples in each experiment. Each data point is the result of a fitted data set, and each color represents a set of fits for all data sets in a single experiment. The average fitting (R^2) for all experiments was 0.98.

Local shape changes in SPN2 with incubation time and the H-bond partner

To understand the nature of the changes occurring around the ligand binding pocket, SHAPE (Merino et al. 2005; Wilkinson et al. 2005; Steen et al. 2011) was performed with SPN2 in the presence of DFHBI or PFP-DFHBI at 10 min or after 2 h incubation at room temperature. Although the results showed a variety of changes in 2′OH exposure over the entire molecule (Fig. 6A), the most prominent differences between DFHBI and PFP-DFHBI in their interaction with SPN2 over time were around the binding pocket (positions 60–75). After

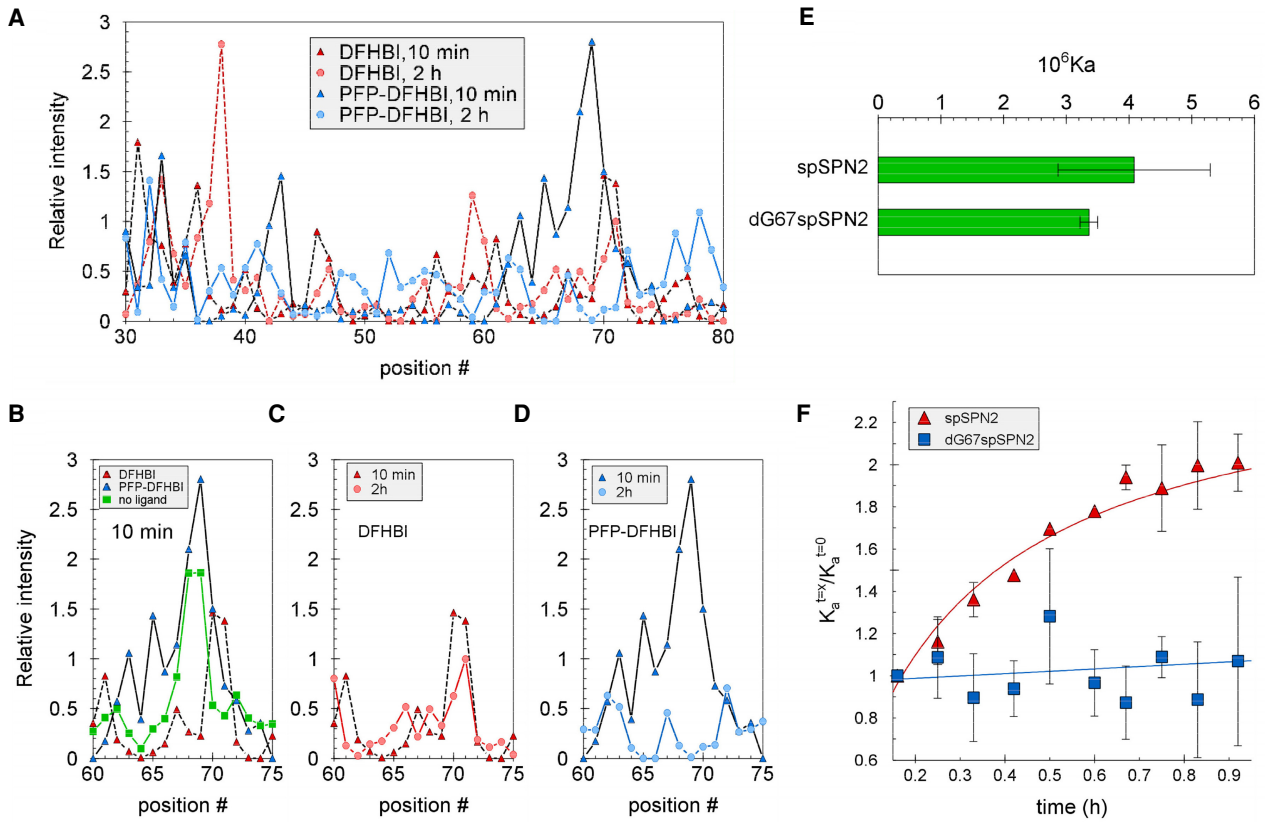

FIGURE 6. Evidence for an initial disruption by PFP-DFHBI around the SPN2 binding pocket entrance followed by structural uniformity around the pocket requiring the 2′OH on G67. (*A–D*) SPN2 was analyzed by SHAPE after 10- and 120-min incubations with DFHBI and PFP-DFHBI in buffer SX. (*A*) Relative intensities at all aptamer positions from incubations for 10 or 120 min with DFHBI or PFP-DFHBI. (*B–D*) Relative intensities in the region around the gateway A after incubation for (*B*) 10 min with DFHBI or PFP-DFHBI, (*C*) 10 or 120 min with DFHBI, or (*D*) 10 or 120 min and PFP-DFHBI. (*E*) The affinities for PFP-DFHBI of spSPN2 and dG67spSPN2 at 10 min. (*F*) Time course of the change in affinity for PFP-DFHBI of SPN2 and SPN2 with dG at position 67 (dG67SPN2).

10 min incubation with either DFHBI or PFP-DFHBI, the region around the gateway A was altered in its exposure to modification by benzoyl cyanide, the SHAPE reagent (Fig. 6B). However, a difference between the effects of these two ligands was observed when 10 min and 2 h incubations were analyzed. Whereas the aptamer shape around the binding pocket changed little with DFHBI over this time period (Fig. 6C), this region appeared destabilized after 10 min with PFP-DFHBI followed by a tightening down after 2 h (Fig. 6D). These results are consistent with the interpretation that PFP-DFHBI disrupts the local RNA structure enabling the aptamer to overcome a local folding energy barrier, which allows formation of a new bond near the ligand binding pocket.

We examined the crystal structure of SPN2 to identify possible candidates for a hypothesized H-bond with the secondary amino group of the gateway adenine. The closest hydroxyl to the gateway amino group is on G67 (G65 in the crystal structure), which is 5.5 Å from the amino nitrogen of the gateway A (Supplemental Fig. S2). This distance is too long to support a hydrogen bond, but we hypothesized that PFP-DFHBI disturbs the aptamer structure around the binding pocket sufficiently to allow a realignment of residues. The result of this disturbance could be the formation of a new H-bond that stabilizes the position of the A over the binding pocket resulting in a more suitable entry site for PFP-DFHBI and an increase in ligand affinity due to the higher k_{on}. To test this hypothesis, we determined the rate of change in affinity of SPN2 with a dG in position 67 in place of G. Replacement of the deoxyribose for ribose at position 67 did not alter ligand affinity (Fig. 6E). However, unlike the aptamer with a 2′ OH at position 67, the aptamer with 2′ deoxy pentose in position 67 did not change in affinity with time (Fig. 6F). Thus, the 2′ OH at position 67 is required for a change in affinity of SPN2.

DISCUSSION

Members of the Spinach aptamer family all possess an adenine in the equivalent gateway position directly outside the ligand pocket entrance (Warner et al. 2014;

Fernandez-Millan et al. 2017). The presence of this A is essential for maintaining high ligand affinities of Spinach and related aptamers as shown here and previously by others (Warner et al. 2014; Fernandez-Millan et al. 2017). The crystal structure shows that the gateway A interacts in a T-stack formation with the methyl group of the imidazole nitrogen in DFHBI (Huang et al. 2014). Such an arrangement should readily be replaced by another purine, either 2AP or G. But, any replacement of the A in the gateway position, including of 2AP, resulted in a decrease in affinity. We suspect that the two other purine replacements, 2AP and G, at position 71 might be displaced by interaction (s) with another portion of the aptamer that leaves them unable to replace A as "lid" for the binding pocket.

Here we provide evidence of an alternative structure for SPN2 with increased ligand affinity, which is achieved because of a local rearrangement of the bases around the ligand pocket initiated by polyfluorophenyl-DFHBI ligands. Our evidence suggests that the new structure is stabilized by a hydrogen bond between the gateway A and the close-by 2′ hydroxyl group of G67. Based on the SHAPE analysis, we speculate that the aptamer rearrangement results from a disturbance at the ligand pocket entrance by the presence of the polyfluorophenyl moieties of the relevant DFHBI analogs. The direct involvement of the amino group on the A in the rearrangement is supported by the observation that C is the only base other than A that enables an increase in affinity with time. This is despite the observation that the affinity of the aptamer with C71 is very low for PFP-DFHBI.

Being in the order of 400 kJ/mol, a single hydrogen bond (Benson 1965; Kerr 1966) is not likely to hold a new structure of a large aptamer such as SPN2 without cooperation from other parts in the molecule. Thus, it is anticipated that this predicted change in structure involves a cooperative rearrangement around the binding pocket as a result of structural perturbation by PFP-DFHBI. The tenuous nature of this proposed structure suggests that it might be sensitive to increased temperature. Indeed, when BRC was incubated at 37°C with PFP-DFBHI, the affinity dropped over time. By comparison, the affinity for DFHBI was stable over 3 h at 37°C (Supplemental Fig. S5). These results are consistent with the hypothesis that PFP-DFHBI disrupts the local structure around the binding site for SPN2. Whereas the proposed disruption enables formation of a G67-A71 hydrogen bond at 23°C, this bond is not sufficiently stable at 37°C and instead of increasing with time, the affinity for PFP-DFHBI decreases.

Two properties of the polyfluorinated phenyl moieties are possible drivers of local structural disruption. First, unlike other halogens, F can form hydrogen bonds, albeit weak (Howard et al. 1996; Bissantz et al. 2010; Dalvit et al. 2014). Second, fluorines are particularly hydrophobic (Bissantz et al. 2010; Mondal and Mahapatra 2010). Either or both properties might be responsible for a local disturbance in the ligand pocket entrance structure. The possibility of a chemical modification of the aptamer that either involves the ligand or is initiated by the ligand is unlikely. First, the change in affinity due to PFP-DFHBI is completely reversible upon melting the SPN2 structure. Second, the change in affinity is not initiated by interaction with DFHBI-1T, which has a trifluoromethyl extension to the imido nitrogen of DFHBI.

The initial structural disturbance caused by the polyfluorophenyl appendage to the ligand is proposed to enable sufficient mobility in the region of the pocket entrance for the gateway A amino group and the G67 2′OH to approach each other and form a hydrogen bond. This bond and the microenvironment in which the base is then located is proposed to shift RNA structure at the pocket entrance to a more receptive structure for PFP-DFHBI entrance into the pocket. Instead of a direct H-bond between the gateway A and G67, other more complicated interactions may occur that involve these groups and others on the RNA. However, the first order nature of the affinity change with time identifies a single interaction as the driving force for increased aptamer affinity for the polyfluorophenyl-DFHBI derivatives. Thus, without evidence of the involvement of other components on the RNA, we propose that interaction with PFP-DFHBI results in the formation of a hydrogen bond between A71 and G67, which promotes a more uniform structure of the pocket entrance.

Analysis of the kinetic parameters behind the affinities of SPN2 for DFHBI and PFP-DFHBI show that the k_{off} is the same for both ligands and does not change with incubation time. Although k_{off} for DFHBI has previously been calculated based on measurements of k_{on} (Han and Lee 2013) this is the first time to our knowledge that k_{off} has been measured experimentally. Measurement of k_{off} requires the availability of a high affinity ligand for SPN2 (PNP-DFHBI) that does not fluoresce when bound to the aptamer. The measured off rates for both ligands after short or long incubation times were very similar and differences did not account for the different affinities of SPN2 for the two ligands or for PFP-DFHBI after an incubation period. The changes in kinetic parameters that are consistent with the changes in affinity between ligands and incubation time were found in k_{on}.

The observed difference between SPN2 binding of PFP-DFHBI and DFHBI in k_{on} and not in k_{off} suggests that the K_a is controlled by the k_{on}. A change in k_{off} would be consistent with a change in the number or type of interactions between aptamer and ligand, such as increased stacking between aptamer and phenyl groups on the ligand that holds the ligand more tightly to the aptamer. In contrast, a change in k_{on} is more consistent with a more readily accessible binding pocket for ligand entry. The values measured for k_{on} of both compounds are $\sim 10^4$ to 10^5 lower than the diffusion-controlled limit of 10^2 to 10^4 $\mu M^{-1}s^{-1}$ (Alberty and Hammes 1958). Our results for k_{on} are in the same order

of magnitude as previously reported for the Chili aptamer (8.2×10^4 $\mu M^{-1}s^{-1}$; Steinmetzger et al. 2019) and almost identical to the k_{on} reported for DFHBI-1T and BRC (1.4×10^{-4} $\mu M^{-1}s^{-1}$; Li et al. 2020). Another reported k_{on} for DFHBI binding to surface-attached Spinach ($6.2 \pm 0.1 \times 10^{-2}$ $\mu M^{-1}s^{-1}$; Han et al. 2013) is about 300-fold higher than the measurements of DFHBI binding to SPN2 and related aptamers in solution. However, all estimates of the k_{on} are orders of magnitude lower than the diffusion-controlled limit. This suggests a large energy barrier to the entry of these compounds into the SPN2 pocket with the additional pentafluorophenyl group of PFP-DFHBI decreasing that barrier by 10–20-fold. The increased rate of binding of PFP-DFHBI compared with DFHBI may be due to the greater disruption in the region around the binding site caused by PFP-DFHBI compared with DFHBI that was detected by SHAPE analysis.

As a broad range of new roles are attributed to RNAs in cells, opportunities will open for regulating cellular activity with small molecule inhibitors. The findings here with the SPN2 and Broccoli aptamers suggest k_{on} is the critical kinetic parameter and that the inclusion of polyfluorophenyl moieties might disrupt a local region of the RNA target at a location such as a bulge or loop. Such disturbance might allow the RNA to overcome a local energy barrier to folding with a resulting alteration in structure and potentially function. It is of interest to note that among small drug pharmaceuticals, fluoro-pharmaceuticals are rapidly increasing in representation such that more than 60% of recently approved pharmaceuticals contain at least one fluorine (Inoue et al. 2020). Many of the current fluoropharmaceuticals have structures that would enable their interactions with RNA, which could contribute to their effectiveness. These observations and our results suggest that the inclusion of polyfluorophenyl groups on RNA-targeting drugs should be explored for the possibility of increasing drug effectiveness.

MATERIALS AND METHODS

Reagents

Buffer IC was formulated to approximate intracellular pH and ionic concentrations based on literature reports for these values (Rorsman et al. 1982; Ammann et al. 1995; Grubbs 2002; Romani 2007, 2013) and contained 13.5 mM NaCl, 150 mM KCl, 0.22 mM Na_2HPO_4, 0.44 mM KH_2PO_4, 120 µM $MgCl_2$, 120 nM $CaCl_2$, 100 µM $MgSO_4$, 20 mM HEPES, pH 7.4. Buffer SX, which was used for the SPN2 aptamer selection (Strack et al. 2013), contained 125 mM KCl, 5mM $MgCl_2$, 40 mM HEPES, pH 7.4. Buffer SB, which was the buffer for BRC selection (Filonov et al. 2014), contained 100 mM KCl, 1 mM $MgCl_2$, 40 mM HEPES, pH 7.4. All buffers were prepared with deionized distilled water and the pHs were measured at 24°C–25°C. Due to the need to dissolve reagents in DMSO, all reaction mixes also contained 5% DMSO. Buffer formulations are shown in Supplemental Table S2. All inorganic chemicals were from Fisher Scientific.

Preparation of RNAs

The SPN2 RNA used in this study contains the sequence of SPN2 (Strack et al. 2013) with the addition of two G's at the 5′ end that are added by T7 polymerase at transcriptional initiation. Sequences of the RNA aptamers and their variants used in this study are shown in Supplemental Table S2. RNAs were prepared by in vitro transcription with the AmpliScribe T7 Flash or T7 High Yield in vitro transcription kits (Epicenter) from templates created by oligonucleotide annealing and PCR amplification. Alternatively, the RNA was prepared by laboratory-made T7 polymerase. BRC and the chemically modified portions of SPN2 were synthesized chemically by Integrated DNA Technologies (IDT). These are identified in Supplemental Table S2.

For SPN2 RNAs with either a 2-aminopurine (2AP) or no purine at position 71, a split construction was used. The two halves of the split SPN2 (sequences specified in Supplemental Table S2) were those used to create the SPN2 RNA in an equivalent way to which the SPN2 RNA was prepared to determine its structure by X-ray crystallography (Warner et al. 2014). One half of each RNA containing either a substitution of 2AP for A21 or with an apurinic pentose sugar at position 21 (Apu) were chemically synthesized by IDT and maintained at −20°C in autoclaved deionized distilled water (ddH_2O) until use. Position A21 in this first half-molecule corresponds to A71 in the full-length SPN2 (Supplemental Table S2). The second RNA molecule half was synthesized as described for the full-length RNA molecule. The two halves were combined in SX buffer, heated to 95°C for 5 min, then slowly cooled to 25°C over a period of 1 h. These reassembled aptamers are referred to as split SPN2 (spSPN2).

Synthesis of imidazole derivatives

The general procedure for the preparation of chemicals in the small molecule library of DFHBI analogs with alternate imido-N extensions was as follows: To the azlactone (0.200 g, 0.711 mmol) in ethanol (10 mL) was added a solution of the primary amine (0.853 mmol) in ethanol (10 mL), followed by potassium carbonate (0.1474 g, 1.07 mmol). The reaction mixture was refluxed for 12 h. After cooling to room temperature, the solvent was removed by evaporation. Water (15 mL) was added, and the pH was adjusted to three using 1 M HCl. The solution was left overnight at 4°C and the resulting precipitated product was captured by filtration. In some instances, additional purification by preparative TLC was required. The products were yellow solids. Each compound resolved as one spot on TLC. NMR and high-resolution mass spectrometry data were consistent with the assigned structures (Supplemental Material).

The spectral properties of the DFHBI and PFP-DFHBI are in Supplemental Table S5. Quantum yields (QY) of DFHBI and PFP-DFHBI were determined in complex with tandem SPN2 relative to acridine orange in SX buffer with 5% DMSO. The results were analyzed using ORIGIN 7 [v7.0552 (B552), www.OriginLab

.com] for absorbance deconvolution and the formula below to determine QY:

$$QY = QY_{ref}\frac{\eta^2}{\eta_{ref}^2}\frac{I}{A}\frac{Aref}{Iref},$$

where η = refractive index, A = absorbance, I = integrated area.

Computational analyses of structure of the aptamer and potential ligands

Images of the SPN2 structure in association with its ligand were prepared from 4ts2.pdb using Pymol (https://pymol.org/2/). The MM2 force field method, available in the ChemBio3D Ultra 12 Suite, was used for calculating the properties of organic molecular models from which the 3D images of DFHBI extension ligands were created. Default parameters for geometry optimizations are used in ChemBio3D until the gradient norm is less than the minimum RMS gradient of 0.100.

Fluorescence measurements

Fluorescence intensities were measured by a Cary Eclipse Spectrofluorometer (Varian) for single time point measurements and a Synergy 2 plate reader (BioTek) for multiple time point measurements.

Determination of affinities

The dissociation constants (K_d) of the aptamer-ligand complexes were determined by measuring the increase in fluorescence with increasing ligand concentration while the aptamer concentration was held constant. SPN2 RNA (0.05 µM) was incubated for various time periods (10 min to 3 h) in the dark at 23°C with various concentrations up to 50 µM DFHBI in buffer SX with 5% DMSO. BRC RNA (0.05 µM) was incubated under the same conditions with buffer SB in place of buffer SX. Fluorescence intensities were measured with $\lambda_{ex} = 485$ nm and $\lambda_{em} = 528$ nm with 20 nm slit widths. The fluorescence data, normalized to the maximum value in each data set, was fit in Microsoft Excel using the Solver Add-in (GRG Non-linear method) and the equation

$$F = F_{min} + (F_{max} \times L^n)/(L^n + K_d^n)$$

(Huang et al. 2014), where F is fluorescence, L is the concentration of ligand, n is the Hill coefficient, and K_d is the binding constant. The fit was calculated by instructing the Solver to minimize the sum of the squares while allowing F_{min}, F_{max}, n, and K_d to vary. K_a was calculated as the inverse of the K_d. For some of the variant aptamers, for which the affinity for ligand was low, n was set to 1 to obtain a proper fit. However, the fits for all data for SPN2 and BRC provided n values close to 1. The compiled n values from these fits are shown in Supplemental Table S6. Samples of titration data are shown in Supplemental Figure S3, and the values obtained from this work are compared with already published results from others in Supplemental Table S7. The reported estimates of K_d vary between reports mainly due to variations in conditions (temperature, buffer salts).

Kinetic measurements

The k_{on} and k_{off} rates for SPN2 with DFHBI or PFP-DFHBI were done by stopped-flow kinetics using a MOS-250 spectrometer linked to a stopped-flow SFM-400 apparatus by a MPS-60 microprocessor unit (Bio-Logic), or using a Cary Eclipse Fluorescence Spectrophotometer. The interaction with either ligand was monitored by fluorescence (excitation at 460 nm and emission at 500 nm). For k_{on} measurements, 20 nM SPN2 was mixed with DFHBI or PFP-DFHBI in 125 mM KCl, 5 mM $MgCl_2$, 40 mM HEPES, 5% DMSO, pH 7.4 at 25°C at final concentrations of 50, 100, 200, 250, 300, 400, 500, or 800 nM. Binding was monitored by the change in fluorescence at 500 nm over the period from 20 msec to 150 sec after mixing. In some experiments, the final concentration of DMSO was 2.5%. For k_{off} rates, PNP-DFHBI was present in excess to replace the dissociated ligand in the SPN2 binding pocket and thereby prevent the reassociation of DFHBI or PFP-DFHBI. PNP-DFHBI does not fluoresce when it binds to SPN2 and competes for binding with both DFHBI and PFP-DFHBI (Supplemental Fig. S4). Mixtures of SPN2 and DFHBI or PFP-DFHBI were mixed with PNP-DFHBI to achieve final concentrations at $t = 0$ of 40 mM HEPES, 125 mM KCl, 5 mM $MgCl_2$, pH 7.4, 5% DMSO, 100 nM SPN2, 20 µM DFHBI or PFP-DFHBI, and PNP-DFHBI at 100 or 200 µM. The dissociation of DFHBI or PFP-DFHBI from SPN2 was monitored by the change in fluorescence at 500 nm during the period of 20 msec to 150 sec. The kinetic data were fit with an exponential function using Costat (version 6.541) to obtain k_{off} and k_{obs}. k_{on} is the slope of the linear transformation $k_{obs} = k_{on} \times [L] + c$, where [L] is the ligand (DFHBI or PFP-DFHBI) concentration and c is a constant.

SHAPE

SPN2 RNA in water was heated to 65°C for 5 min, cooled to room temperature then diluted into buffer SX at 37°C to 9.9 µM RNA, with and without 10 µM ligand. The mixtures were incubated at 65°C for 10 min. The RNA was reacted with or without 5 mM benzoyl cyanide in buffer SX with 4.9% DMSO, reverse transcription was done with Thermo Fisher Superscript IV with 0.5 mM of each nucleotide triphosphate (NTP) and a 5′ hexachloro-fluorescein (HEX) end-labeled primer (TTTTGTTTATTCTTTT). A G-ladder was created using the same primer 5′ labeled with 6-carboxyfluorescein (6FAM) and RT reactions that included 0.5 mM ddGTP. Completed reactions were ethanol precipitated and resuspended in deionized formamide (Hi-Di Formamide, Thermo Fisher) with the G-ladders. Fragmentation analysis of the resulting cDNAs was performed on an Applied Biosystems 3730 DNA Analyzer by the DNA facility (Iowa State University). The data was normalized using the QuShape v. 1.0 software with the following calculation:

$$P_{add}(i) = \frac{P_{term}^{+}(i) - \alpha \cdot P_{term}^{-}(i)}{1 - \alpha \cdot P_{term}^{-}(i)},$$

where

$$P_{term}(i) = P_{add}(i) - P_{add}(i) \cdot P_{spont}(i) + P_{spont}(i),$$

where $P_{term}^{+}(i)$ and $P_{term}^{-}(i)$ are the probabilities of primer termination at nucleotide i in reaction mixes with (+) and without (–) benzoyl cyanide. The parameter α accounts for scaling differences

between the spontaneous termination probabilities in the two reactions (Karabiber et al. 2013).

SUPPLEMENTAL MATERIAL

Supplemental material is available for this article.

COMPETING INTEREST STATEMENT

M.N.H. is the owner of Aptalogic Inc.

ACKNOWLEDGMENTS

We thank Jonathan Beasley for synthesizing DFHBI, Joshua Alterman for preparing a batch of PNP-DFHBI, Aleksei Ananin for help with MS measurements, Ilchung Shin and Judhajeet Ray for contributing data, Scott Nelson for help with stopped-flow measurements, Richard Honzatko for useful discussion, and Walter Moss for critiquing an early version of the manuscript. This work was supported by the National Institutes of Health (grant number R21AI114283) (chemistry) and Aptalogic Inc. (molecular biology).

Author contributions: The chemical library was prepared by I.M.G. with oversight from G.A.K. The majority of the data was collected and individually analyzed by S.A. with contributions from M.I. and L.B. M.N.H. compiled and evaluated the data, developed the hypothesis, and directed the work progress. L.B. discovered the change in aptamer affinity with time, M.I. proposed the gateway A as important, and M.N.H. proposed the G67 OH group. M.N.H. wrote the manuscript with contributions from all coauthors.

Received October 5, 2021; accepted March 11, 2022.

REFERENCES

Ageely EA, Kartje ZJ, Rohilla KJ, Barkau CL, Gagnon KT. 2016. Quadruplex-flanking stem structures modulate the stability and metal ion preferences of RNA mimics of GFP. *ACS Chem Biol* **11:** 2398–2406. doi:10.1021/acschembio.6b00047

Alberty RA, Hammes GG. 1958. Application of the theory of diffusion-controlled reactions to enzyme kinetics. *J Phys Chem* **62:** 154–159. doi:10.1021/j150560a005

Ammann H, Noel J, Tejedor A, Boulanger Y, Gougoux A, Vinay P. 1995. Could cytoplasmic concentration gradients for sodium and ATP exist in intact renal cells? *Can J Physiol Pharmacol* **73:** 421–435. doi:10.1139/y95-055

Benson SW. 1965. III—bond energies. *J Chem Educ* **42:** 502. doi:10.1021/ed042p502

Bissantz C, Kuhn B, Stahl M. 2010. A medicinal chemist's guide to molecular interactions. *J Med Chem* **53:** 5061–5084. doi:10.1021/jm100112j

Dalvit C, Invernizzi C, Vulpetti A. 2014. Fluorine as a hydrogen-bond acceptor: experimental evidence and computational calculations. *Chemistry (Easton)* **20:** 11058–11068. doi:10.1002/chem.201402858

Dethoff EA, Chugh J, Mustoe AM, Al-Hashimi HM. 2012. Functional complexity and regulation through RNA dynamics. *Nature* **482:** 322–330. doi:10.1038/nature10885

Fernandez-Millan P, Autour A, Ennifar E, Westhof E, Ryckelynck M. 2017. Crystal structure and fluorescence properties of the iSpinach aptamer in complex with DFHBI. *RNA* **23:** 1788–1795. doi:10.1261/rna.063008.117

Filonov GS, Moon JD, Svensen N, Jaffrey SR. 2014. Broccoli: rapid selection of an RNA mimic of green fluorescent protein by fluorescence-based selection and directed evolution. *J Am Chem Soc* **136:** 16299–16308. doi:10.1021/ja508478x

Grubbs RD. 2002. Intracellular magnesium and magnesium buffering. *Biometals* **15:** 251–259. doi:10.1023/A:1016026831789

Han SR, Lee S-W. 2013. *In vitro* selection of RNA aptamer specific to *Salmonella* Typhimurium. *J Microbiol Biotechnol* **23:** 878–884. doi:10.4014/jmb.1212.12033

Han KY, Leslie BJ, Fei J, Zhang J, Ha T. 2013. Understanding the photophysics of the spinach-DFHBI RNA aptamer-fluorogen complex to improve live-cell RNA imaging. *J Am Chem Soc* **135:** 19033–19038. doi:10.1021/ja411060p

Howard JAK, Hoy VJ, O'Hagan D, Smith GT. 1996. How good is fluorine as a hydrogen bond acceptor? *Tetrahedron* **52:** 12613–12622. doi:10.1016/0040-4020(96)00749-1

Huang H, Suslov NB, Li N-S, Shelke SA, Evans ME, Koldobskaya Y, Rice PA, Piccirilli JA. 2014. A G-quadruplex-containing RNA activates fluorescence in a GFP-like fluorophore. *Nat Chem Biol* **10:** 686–691. doi:10.1038/nchembio.1561

Ilgu M, Ray J, Bendickson L, Wang T, Geraskin IM, Kraus GA, Nilsen-Hamilton M. 2016. Light-up and FRET aptamer reporters; evaluating their applications for imaging transcription in eukaryotic cells. *Methods* **98:** 26–33. doi:10.1016/j.ymeth.2015.12.009

Inoue M, Sumii Y, Shibata N. 2020. Contribution of organofluorine compounds to pharmaceuticals. *ACS Omega* **5:** 10633–10640. doi:10.1021/acsomega.0c00830

Karabiber F, McGinnis JL, Favorov OV, Weeks KM. 2013. QuShape: rapid, accurate, and best-practices quantification of nucleic acid probing information, resolved by capillary electrophoresis. *RNA* **19:** 63–73. doi:10.1261/rna.036327.112

Kerr JA. 1966. Bond dissociation energies by kinetic methods. *Chem Rev* **66:** 465–500. doi:10.1021/cr60243a001

Li X, Kim H, Litke JL, Wu J, Jaffrey SR. 2020. Fluorophore-promoted RNA folding and photostability enables imaging of single Broccoli-tagged mRNAs in live mammalian cells. *Angew Chem Int Ed Engl* **59:** 4511–4518. doi:10.1002/anie.201914576

Mandal M, Lee M, Barrick JE, Weinberg Z, Emilsson GM, Ruzzo WL, Breaker RR. 2004. A glycine-dependent riboswitch that uses cooperative binding to control gene expression. *Science* **306:** 275–279. doi:10.1126/science.1100829

Merino EJ, Wilkinson KA, Coughlan JL, Weeks KM. 2005. RNA structure analysis at single nucleotide resolution by selective 2'-hydroxyl acylation and primer extension (SHAPE). *J Am Chem Soc* **127:** 4223–4231. doi:10.1021/ja043822v

Mondal T, Mahapatra S. 2010. Photophysics of fluorinated benzene. I. Quantum chemistry. *J Chem Phys* **133:** 084304. doi:10.1063/1.3465555

Paige JS, Wu KY, Jaffrey SR. 2011. RNA mimics of green fluorescent protein. *Science* **333:** 642–646. doi:10.1126/science.1207339

Priyakumar UD. 2010. Atomistic details of the ligand discrimination mechanism of S_{MK}/SAM-III riboswitch. *J Phys Chem B* **114:** 9920–9925. doi:10.1021/jp1042427

Romani A. 2007. Regulation of magnesium homeostasis and transport in mammalian cells. *Arch Biochem Biophys* **458:** 90–102. doi:10.1016/j.abb.2006.07.012

Romani AMP. 2013. Magnesium homeostasis in mammalian cells. *Met Ions Life Sci* **12:** 69–118. doi:10.1007/978-94-007-5561-1_4

Rorsman P, Berggren PO, Hellman B. 1982. Manganese accumulation in pancreatic β-cells and its stimulation by glucose. *Biochem J* **202:** 435–444. doi:10.1042/bj2020435

Song W, Strack RL, Svensen N, Jaffrey SR. 2014. Plug-and-play fluorophores extend the spectral properties of spinach. *J Am Chem Soc* **136:** 1198–1201. doi:10.1021/ja410819x

Steen K-A, Siegfried NA, Weeks KM. 2011. Selective 2′-hydroxyl acylation analyzed by protection from exoribonuclease (RNase-detected SHAPE): direct analysis of covalent adducts and of nucleotide flexibility in RNA. *Nat Protoc* **6:** 1683–1694. doi:10.1038/nprot.2011.373

Steinmetzger C, Bessi I, Lenz A-K, Höbartner C. 2019. Structure–fluorescence activation relationships of a large Stokes shift fluorogenic RNA aptamer. *Nucleic Acids Res* **47:** 11538–11550. doi:10.1093/nar/gkz1084

Stoddard CD, Montange RK, Hennelly SP, Rambo RP, Sanbonmatsu KY, Batey RT. 2010. Free state conformational sampling of the SAM-I riboswitch aptamer domain. *Structure* **18:** 787–797. doi:10.1016/j.str.2010.04.006

Strack RL, Disney MD, Jaffrey SR. 2013. A superfolding Spinach2 reveals the dynamic nature of trinucleotide repeat-containing RNA. *Nat Methods* **10:** 1219–1224. doi:10.1038/nmeth.2701

Suess B, Fink B, Berens C, Stentz R, Hillen W. 2004. A theophylline responsive riboswitch based on helix slipping controls gene expression *in vivo*. *Nucleic Acids Res* **32:** 1610–1614. doi:10.1093/nar/gkh321

Warner KD, Chen MC, Song W, Strack RL, Thorn A, Jaffrey SR, Ferré-D'Amaré AR. 2014. Structural basis for activity of highly efficient RNA mimics of green fluorescent protein. *Nat Struct Mol Biol* **21:** 658–663. doi:10.1038/nsmb.2865

Warner KD, Sjekloća L, Song W, Filonov GS, Jaffrey SR, Ferré-D'Amaré AR. 2017. A homodimer interface without base pairs in an RNA mimic of red fluorescent protein. *Nat Chem Biol* **13:** 1195. doi:10.1038/nchembio.2475

Wilkinson KA, Merino EJ, Weeks KM. 2005. RNA SHAPE chemistry reveals nonhierarchical interactions dominate equilibrium structural transitions in $tRNA^{Asp}$ transcripts. *J Am Chem Soc* **127:** 4659–4667. doi:10.1021/ja0436749

MEET THE FIRST AUTHOR

Sharif Anisuzzaman

***Meet the First Author(s)* is a new editorial feature within *RNA*, in which the first author(s) of research-based papers in each issue have the opportunity to introduce themselves and their work to readers of *RNA* and the RNA research community. Sharif Anisuzzaman is the first author of this paper, "Ligands with polyfluorophenyl moieties promote a local structural rearrangement in the Spinach2 and Broccoli aptamers that increases ligand affinities." Sharif obtained master's degrees in pharmaceutical sciences at Jahangirnagar University, Bangladesh and in biochemistry at Tennessee State University. He is now a PhD student in the laboratory of Dr. Marit Nilsen-Hamilton at Iowa State University, working on structural changes of ribonucleic acid (RNA) aptamers upon binding their small molecule ligands.**

What are the major results described in your paper and how do they impact this branch of the field?

In this work, we investigated the interaction of the Spinach2 and Broccoli aptamers with a library of small molecule ligands with various extensions from the imido nitrogen of DFHBI (3,5-difluoro-4-hydroxybenzylidene imidazolinone) that reach out from the Spinach2/Broccoli ligand binding pockets. Studies of the interaction of these compounds with the aptamers revealed that polyfluorophenyl-modified ligands initiate a slow change in aptamer affinity that takes an extended time (half-life of ~40 min) to achieve. The change in affinity appears to involve an initial disruption of the entrance to the ligand pocket followed by a gradual transition to a defined structure for which the most likely driving force is an interaction of the gateway adenine with a nearby 2′OH group.

Fluorine-containing small molecule drugs are increasingly important in pharmaceuticals, and RNA is emerging as a potential target. This study suggests that inclusion of polyfluorophenyl groups on RNA-targeting drugs should be explored for the possibility of increasing drug effectiveness. We speculate that polyfluorophenyl modifications of potential drugs might increase the drug's ability to disrupt local structure and promote RNA remodeling, preferably around the drug.

What led you to study RNA or this aspect of RNA science?

During my undergraduate training in pharmacy, studying the mechanisms of action of drugs was my favorite subject. To understand these interactions at the molecular level, I decided to switch my area from pharmacy to biochemistry. This led me to choose a research area in the interaction of small molecules with RNA.

During the course of these experiments, were there any surprising results or particular difficulties that altered your thinking and subsequent focus?

Replacement of adenine at 71 positions of Spinach2 RNA aptamer with an apurinic base decreased binding affinity by 100-fold and there is no increase in binding affinity over time. This observation led to thinking about this position and further exploration of the

Continued

structural changes of the aptamer as it interacted with the polyfluorophenyl-modified ligands.

What are some of the landmark moments that provoked your interest in science or your development as a scientist?

My parents encouraged me to choose science during school. They helped me in my decision making process by sharing their values on science and discussed the various opportunities in this field as a scientist.

If you were able to give one piece of advice to your younger self, what would that be?

Improve my communication and writing skill; science is not all about laboratory work, communication is also important. Effective communications from peers to a general audience promotes support for science and encourages more informed decision making at all levels.

Are there specific individuals or groups who have influenced your philosophy or approach to science?

Group meetings with laboratory members and collaborators have improved my skills in sharing ideas, explaining science, and understanding their ideas and feedback.

What are your subsequent near- or long-term career plans?

In the future, I would like to further explore the structural analysis of 2′ FY-RNA and ssDNA aptamers and their applications in biosensors.